PHYSICAL REVIEW E **74**, 031502 (2006)

Supercooled water relaxation dynamics probed with heterodyne transient grating experiments

Andrea Taschin,[1,2] Paolo Bartolini,[1,2] Roberto Eramo,[1,2,3] and Renato Torre[1,2,3]
[1]*European Laboratory for Non-Linear Spectroscopy (LENS), Università di Firenze, Via N. Carrara 1, I-50019 Sesto Fiorentino, Firenze, Italy*
[2]*INFM-CRS-Soft Matter (CNR), c/o Università la Sapienza, Piazzale Aldo Moro 2, I-00185, Roma, Italy*
[3]*Dipartimento di Fisica, Università di Firenze, Via Sansone 1, I-50019 Sesto Fiorentino, Firenze, Italy*
(Received 22 February 2006; published 13 September 2006)

We report results from a heterodyne-detected transient grating experiment on liquid and supercooled water in a wide temperature range, from −17.5 to 90 °C. The measured signal covers an extremely large time window with an excellent signal-to-noise ratio that enables the investigation in a single experiment of the sound speed and attenuation, thermal diffusivity, and temperature dependence of the dielectric constant. The experimental data clearly show the effect of the density and the temperature fluctuations on the water dielectric function. In order to describe the experimental results, we introduce a comprehensive hydrodynamic model taking into account the coupled density and temperature variables and their relevance in the definition of the spontaneous and forced dielectric variations. We use this model to describe the measured signal in transient grating experiments, including the heating and the electrostrictive sources produced by the laser excitation. The fitting procedure enables the safe extraction of several dynamic proprieties of liquid and supercooled water: the sound velocity and its damping, the thermal diffusivity, and the ratio between the dielectric thermodynamic derivatives. The measured parameters are compared to the literature data and discussed in the complex scenario of water physics.

DOI: 10.1103/PhysRevE.74.031502 PACS number(s): 61.20.Lc, 78.47.+p, 78.40.Dw, 61.20.Ne

I. INTRODUCTION

Water is one of the most relevant substances in the universe, and its importance extends from basic science to many technical applications [1,2]. Despite the paramount interest, several chemical-physical properties of liquid water remain still to be clarified [3]. In particular, in the supercooled phase several phenomena exhibit an anomalous dependence on temperature [4] that require further research investigations [5]. It is still unclear if the temperature singularity affects also acoustic propagation and heat diffusion phenomena.

Acoustic phenomena in liquid water have been discussed in many research papers (see [4,6] and references therein). Between the several anomalous behaviors of the propagation of sound in water, a particularly striking effect is the steep decrease of the adiabatic sound velocity with decreasing temperatures, while a normal liquid shows the opposite trend. This effect is a purely thermodynamic phenomenon, being connected with the temperature variation of the thermodynamic parameters (density, adiabatic compressibility, and specific heat). Dynamic processes are responsible for the positive dispersion that is observed in the high-frequency/wave-vector range [7–10]. In the low-frequency range, where the structural relaxation cannot be effective, the dispersion of sound is still unclear. The comparison between the ultrasonic and the light scattering measurements may suggest the existence of a negative dispersion (sound velocity would decrease with increasing frequency) in the supercooled phase [11,12], but the existence of such anomalous dispersion has never been clearly proved or disproved. Further sound velocity measurements, in the intermediate frequency region, could give valuable information on this aspect.

The thermal diffusivity of liquid water is another relevant parameter but the corresponding relaxation times are difficult to measure; to our knowledge, there is just one experiment in the supercooled phase where it was measured [13]. These data need to be confirmed and extended.

Acoustic and thermal processes in water can be investigated by a transient grating experiment (TG). During the last years these experiments have been used extensively and successfully for probing the dynamics of supercooled liquids [14–20]. This time-resolved spectroscopic tool is able to probe a very broad time window, typically from 10^{-9} to 10^{-3} s, covering with a single experiment a dynamic range hardly explored by other methods. With this technique it is possible to gain relevant information on the low-frequency range of the acoustic propagation and on the slow thermal relaxation phenomena.

Experimental [17–24] and theoretical [25–30] investigations show that an accurate definition of the signal measured in a TG experiment is crucial for its interpretation, as many contributions, coming from several excited material modes, have to be taken into account. The investigation of the TG signal for liquid water has been introduced in few preliminary works [19,21,22], where it has been shown that a comprehensive model of the signal is fundamental in order to safely extract the physical information.

We performed a heterodyne-detected TG experiment on bulk water over a very wide temporal and temperature range. The measured signal shows the acoustic processes and thermal relaxation with an extraordinary signal-to-noise ratio. The quality and extension of the data require an improvement of TG signal definition based on an extended hydrodynamic model. The signal model, defined in this paper, enables the complete fit of the data, without introducing phenomenological fitting parameters, and the safe extraction of the acoustic and thermal proprieties of water.

The work is organized as follows: in the first section we recall the basic description of the TG experiment with the

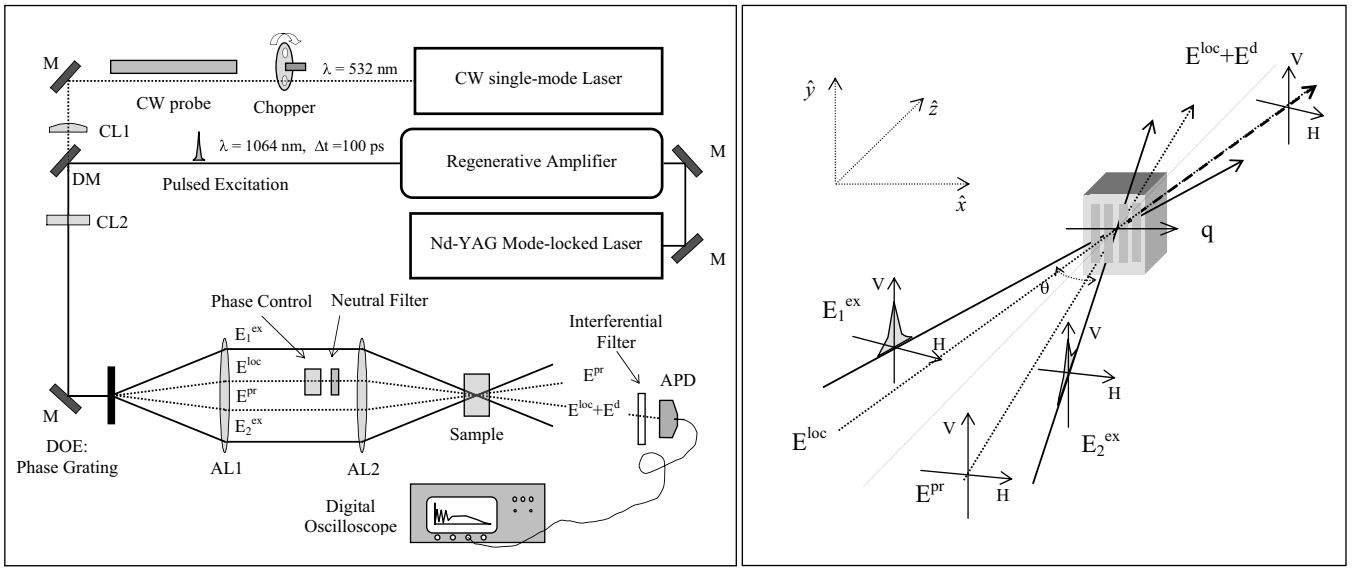

FIG. 1. In the first box we show the experimental setup, including the laser system. M are the mirrors; CL1,2, the cylindrical lenses DM a dichroic mirror; DOE is the diffractive optic element; AL1,2, the achromatic lenses and APD is an avalanche photodiode. In the second box we report the sketch of the polarization configuration and beam directions. E_1^{ex} and E_2^{ex} are the excitation laser pulses and E^{pr} and E^{d} are the probing and diffracted beams, respectively. The optical heterodyne detection is obtained with the local field, E^{loc}. For each beam the possible polarization directions are reported. In particular in the present work we used equal direction of polarizations for the two excitation fields (VV or HH) and for the probe and diffracted beam (again VV or HH). The measured polarization of the diffracted beam is selected by the polarization of the local field.

definitions of response function and measured signal. In Sec. III we report the experimental data with a simple discussion. In Sec. IV we introduce a hydrodynamic model necessary to describe the TG data and extract the water properties. In Sec. V we analyze the TG data and compare them with the literature data. Finally we discuss this work in the present scenario of water results and models.

II. THE TRANSIENT GRATING EXPERIMENTS

The TG experiment is a nonlinear spectroscopic technique that can be classified in the general framework of four-wave-mixing spectroscopy [31,32]. In particular, we are utilizing laser pulses that do not have any electronic resonance with the material so that the Born-Oppenheimer approximation applies [33], and a separation between the electronic effects and the nuclear phenomena can be introduced in the description of the field-matter interaction. According to this approximation the TG experiment can be divided in two separated processes: excitation and probing [17,34,35]. The excitation (see Fig. 1) is produced by two high-power laser pulses, described by $\mathbf{E}_{1,2}^{ex}=E(t)\hat{\mathbf{e}}^{(1,2)}\cos(\mathbf{k}_{1,2}\cdot\mathbf{r}-\omega_l t)$, obtained by dividing a single pulsed laser beam, interfering and producing an impulsive, spatially periodic variation of the dielectric constant, $\delta\epsilon_{ij}(\mathbf{r},t)$, inside the sample; this spatial variation is characterized by a wave vector $\mathbf{q}$, where $\mathbf{q}=\mathbf{k}_1-\mathbf{k}_2=\hat{\mathbf{q}}(2\omega_l/c)\sin\theta/2$. A second cw laser beam, described by $E_p\hat{\mathbf{e}}^{(p)}\cos(\mathbf{k}_p\cdot\mathbf{r}-\omega t)$, typically of different wavelength, is acting as a probe. It impinges on the induced grating at the Bragg angle producing a diffracted beam, spatially separated from the pump and the probe beams. This diffracted beam is the signal measured in a TG experiment, yielding the dynamic information from the relaxing grating. The complete description of TG experiments can be found in numerous review papers, see, for example [20,21,32]. In this section we quote only the final expressions.

When heterodyne detection is employed [17,36,37], the transient grating diffracted field is superimposed, at the detector, to a reference beam, the *local field*, with the same frequency of the probe beam, and in phase with it; the resulting signal is

$$S^{HD}(t) \propto \delta\epsilon_{ij}(t) \propto R_{ijkl}(t), \tag{1}$$

where the Cartesian indexes i and j define the polarizations of the local and of the probe fields, k and l define the polarizations of the pump fields, $\delta\epsilon_{ij}$ is the laser induced modification in the dielectric constant, and R_{ijkl} the response function of the system, that defines the dynamical properties of the experimental observable. Both $\delta\epsilon_{ij}$ and R_{ijkl} are spatial Fourier components corresponding to the exchanged wave vector $\mathbf{q}$, i.e., the grating wave vector. Hence the heterodyne-detected TG signal (HD-TG) measures directly and linearly the relaxation processes defined by the tensor components of the response function. Choosing appropriate polarizations for all the fields we are able to select a single component of the tensor. If we have all the fields characterized by vertical polarization, i.e., the y-axis in Fig. 1, only the R_{yyyy} element will be selected and hence the measured signal will be $S^{HD}_{VVVV}\propto R_{yyyy}$, where we introduced the subscript V for vertical in analogy with the light scattering terminology. Another choice could be $i=j=x$ and $k=l=y$: in this case only the R_{xxyy} element would be selected and hence for the measured signal we would have $S^{HD}_{HHVV}\propto R_{xxyy}$, where now the subscript H

stands for horizontal polarization. The different response components are generally characterized by different relaxation processes [18,23,24,27–29], where both translational and rotational degrees of freedom are involved. The effect of rotational dynamics can be experimentally investigated by a comparison between S^{HD}_{VVVV}, S^{HD}_{HHVV}, and S^{HD}_{VVHH} HD-TG signals. The condition $S^{HD}_{VVVV}=S^{HD}_{HHVV}$, i.e., the absence of birefringence for a given (e.g., *V*) pump configuration is not sufficient alone, as the signal could be dependent on the pump direction relative to the scattering plane, as happen when rototranslational coupling is effective [18,24]. But when we have also $S^{HD}_{VVHH}=S^{HD}_{VVVV}$, we can be confident that orientational dynamics should not be relevant. In any case, the ultimate criterion is how well the adopted dynamical model fits the experimental findings.

The response function contains in general a large amount of information about the system dynamics, and an *ab initio* calculation is a tremendous task that can be carried out only in a limited number of cases [31,33]. Fortunately, in our case the response function can be obtained by following an alternative approach: since we are considering a liquid sample, we first express the dielectric function through the hydrodynamic variables, taking properly into account the effect of the excitation fields on them; we can then calculate the dynamic of the induced grating via the hydrodynamic equations. This procedure, already followed in previous works [14,17,18,20–25,27–30,34], has been originally developed for the interpretation of light scattering (LS) experiments [38], where the signal is defined by the spontaneous dielectric fluctuation. Indeed, the TG experiment measures, in the time domain, the same dynamic properties than a LS experiment measures in the frequency domain, with the difference that the dielectric variations are in the TG case forced by the electromagnetic fields. So, for both experiments the detected signals are determined by the same hydrodynamic equations, even if different initial conditions are involved.

In the hydrodynamic approach the system is described by using only a few variables. The excitation forces drive these out of equilibrium and the response function describes how the system relaxes back to the equilibrium state, i.e., the relaxation of the excited "modes" in the material. These density, temperature, and orientational modes modify the dielectric constant and finally the TG signal. Which modes are indeed excited and effective in defining the dielectric response depends on the specific system under investigation, and has to be ultimately inferred by the experimental results.

III. EXPERIMENTAL RESULTS

The experimental details concerning the laser and the optical setup are extensively reported in [17], here we recall only the main features in order to make clear the present TG data and results. The lasers and the optical setup used to realize the HD-TG experiment are reported in Fig. 1. The excitation is produced by two infrared pulses at 1064 nm wavelength, 100 ps duration, 35 μJ energy, and with a repetition rate of 100 Hz. The pulses are generated by an amplified laser system: a mode-locked Nd-YAG laser (Antares-Coherent) followed by a regenerative Nd-YAG cavity (*R*3800-Spectra Physics). The probing beam, at 532 nm wavelength with 6 mW averaged power after chopping, is produced by a diode-pumped intracavity-doubled Nd-YVO (Verdi-Coherent); this is a cw single-mode laser characterized by an excellent intensity stability with a low and flat noise-intensity spectrum. The beam intensities and polarizations are controlled by half-wave plates and polarizers. We use a phase grating as a diffractive optical element (DOE) made by Edinburgh Microoptics to diffract both laser fields. The excitation grating induced in the sample is the mirror image of the enlightened DOE phase pattern and it is extended in the q direction ($\approx$5 mm); vice versa the probing beam is focalized in a circular spot ($\approx$0.5 mm in diameter). The use of a DOE improves substantially the TG experiments [17,36,37]. The HD-TG signal, after optical filtering, is measured and recorded by the optical input (dc −2.5 GHz bandwidth) of a Tektronix oscilloscope with a limiting bandwidth of 4 GHz and a sampling rate of 20 Gs/s.

Supercooling bulk water is not a trivial task and only a very pure sample can reach and maintain this condition. We performed the measurements on a sealed ampoule of cylindrical shape, prepared for pharmaceutical purposes by Collalto company, that allows one to reach a temperature of −17 °C. In the experimental setup, the sample temperature is controlled by a homemade cryostat with a stability of 0.1 °C. The ampoule is inserted into an aluminum holder fixed to the cold plate of a Peltier cooler; the temperature is controlled by a platinum thermoresistance in thermal contact with the aluminum holder. To limit optical distortions due to the ampoule shape, the scattering plane contains the ampoule axis, and is thus rotated 90° with respect to our previous configuration [17].

In liquids and supercooled water we found $S^{HD}_{VVVV}=S^{HD}_{HHVV}=S^{HD}_{VVHH}$, indicating the absence of rotational effects in the induced grating. Indeed, water shows a birefringence signal, the one measured by the optical Kerr effect spectroscopy [5], but this signal is very weak, and evolves on an extremely short time scale; it is thus completely negligible on the present TG time window. According to these experimental results, the water TG response is not affected by birefringence contributions and hence the study of the relatively slow dynamics of water can be worked out neglecting any polarization effects.

We report in Fig. 2 the HD-TG data at $q=0.63$ μm^{-1} with the polarization configuration of pumps, probe, and detection beams orthogonal to the scattering plane (called in the previous works VVVV configuration). As expected on the basis of the previous studies, the data shows a damped oscillation produced by the acoustic phonon superimposed on a slow exponential decay, generated by thermal diffusion. The two processes correspond to momentum flow and to heat flow mechanisms, and drive the system towards thermal equilibrium. Even a simple look at the temperature dependence of the signal features gives a clear indication of the anomalous behavior of the water TG signal. In fact, the amplitude of thermal decay vanishes at a temperature of about 0 °C and changes sign for lower temperatures in the supercooled phase.

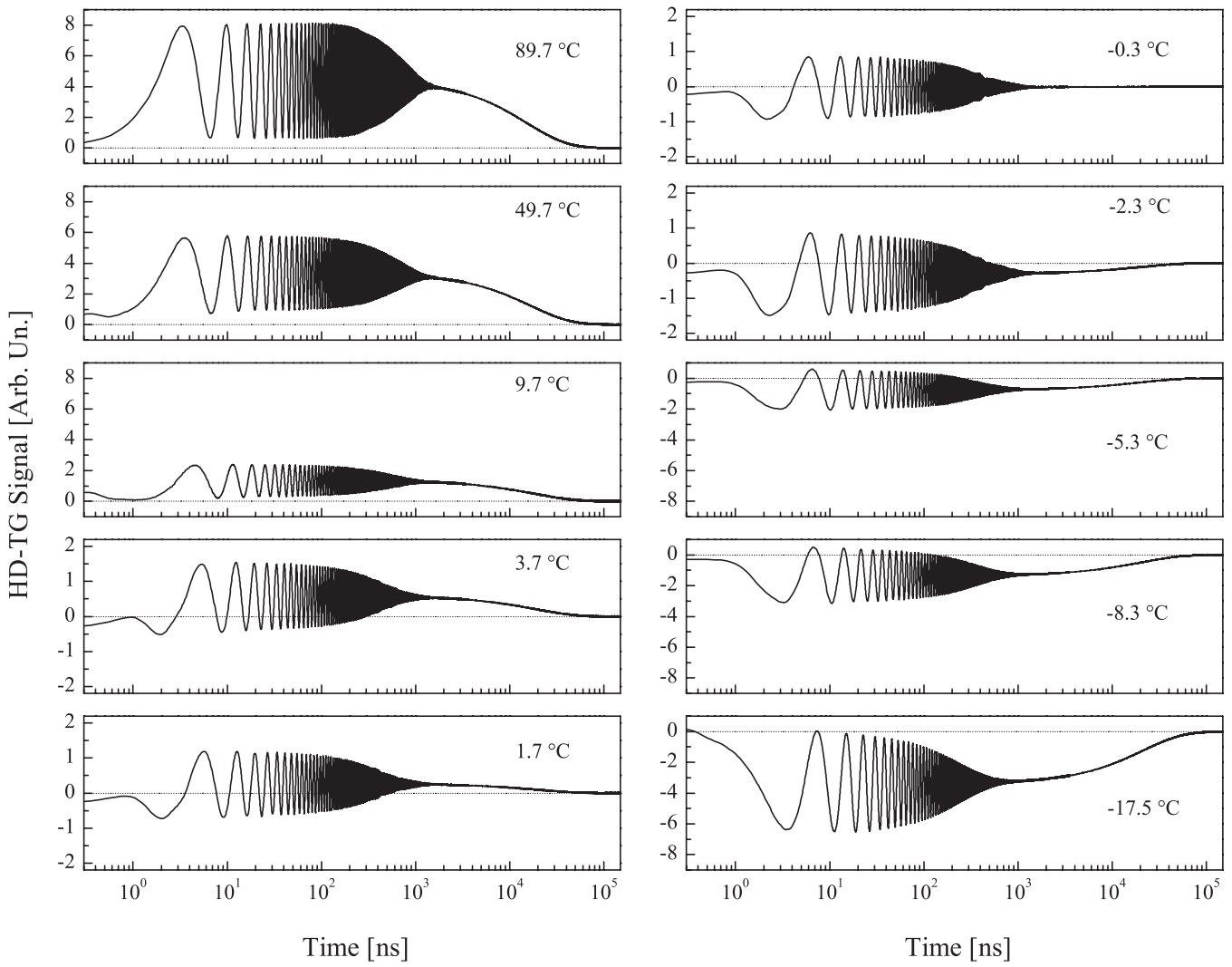

FIG. 2. HD-TG data. HD-TG data on water at $q=0.630\ \mu m^{-1}$ at several temperatures. The data show acoustic oscillations with almost temperature independent damping rate and slow thermal exponential decay. In particular the amplitude of thermal mode vanishes at a temperature of 0 °C and changes sign for lower temperatures.

IV. HYDRODYNAMIC MODELS

As we recall in Sec. II, the TG signal is defined by the laser induced dielectric modification and the following dynamic processes vs equilibrium. These phenomena can be described by the appropriate hydrodynamic model. The definition of the relevant hydrodynamic observable is indeed the starting problem.

In liquid and supercooled water there are two main hydrodynamic variables, as recognized in previous LS [7,11,39] and TG experiments [19,21,22]:

$$\delta\epsilon = \left(\frac{\partial\epsilon}{\partial\rho}\right)_T \delta\rho + \left(\frac{\partial\epsilon}{\partial T}\right)_\rho \delta T, \tag{2}$$

where $\delta\rho$ and δT are the variations, with respect to the equilibrium values, ρ_o and T_o, of the local density and temperature, and the derivatives are found experimentally from the temperature and density variation of ϵ in an equilibrium fluid.

In a more general hydrodynamic model, the orientational variables should be included [29]. This can be obtained introducing an additive term in Eq. (2) that describes the average local orientational distribution of the liquid molecules. As previously reported, we found experimentally that for this HD-TG experiment in water, both in the supercooled and in the ordinary phases, there are not relevant birefringence effects so this term can be neglected.

Vice versa the contribution of the δT-term in water sample cannot be neglected. In particular in a TG experiment the effect of this δT-term can be very evident [19,21,22]. In fact, on the basis of simple thermodynamic considerations, we can express the density and temperature derivative of ϵ using the index of refraction, n, pressure, and temperature derivatives:

$$\left(\frac{\partial\epsilon}{\partial\rho}\right)_T = \frac{2n}{\rho\chi_T}\left(\frac{\partial n}{\partial P}\right)_T, \tag{3}$$

$$\left(\frac{\partial \epsilon}{\partial T}\right)_{\rho} = 2n\left[\left(\frac{\partial n}{\partial T}\right)_{P} + \frac{\alpha}{\chi_T}\left(\frac{\partial n}{\partial P}\right)_{T}\right]. \tag{4}$$

If we focus on the slow dynamics, corresponding to the TG signal at long times after the complete damping of the sound wave often reported as thermal TG, the liquid fluctuations can be taken as isobaric. Hence the $\delta P=[\delta\rho+\alpha\rho_o\delta T]c_s^2/\gamma \approx 0$, and the density evolution can be taken proportional to the temperature evolution, via the α coefficient: $\delta\rho = -\alpha\rho_o\delta T$. So if we substitute Eqs. (3) and (4) in Eq. (2), the pressure derivative terms cancel each other in the isobaric regime giving

$$\delta\epsilon(t) = 2n\left(\frac{\partial n}{\partial T}\right)_{P}\delta T(t). \tag{5}$$

For water the refractive index as a function of temperature has a maximum around 0 °C and hence the multiplicative factor in Eq. (5) reduces to zero the signal around this temperature. This simple expression of the TG signal explains the disappearance of the slow dynamics in the TG experimental results.

Clearly, the TG signal shows other dynamical contributions that must be properly taken into account in the physical model.

Several hydrodynamic models have been introduced in order to address the relaxation phenomena measured by time-resolved TG spectroscopy in liquid sample [15,23,26–30], but only few consider the δT-term [19,21,22,25]. In particular we want to recall the work of Desai *et al.* [25]. In this work the response function has been calculated using the Navier-Stokes equations with the presence of a single excitation force due to the heat deposited in the sample by the laser absorption. This response function defines the thermal grating contribution [i.e., impulsive stimulated thermal scattering (ISTS) [14,29]] to the TG signal inclusive of the δT-term. The relevance of such a term in the thermal grating experiments has been extensively reviewed in [21]. Subsequently, Terazima [22] investigated the importance of the δT-term performing TG experiments in different liquids and utilizing a hydrodynamic model equivalent to that introduced in Ref. [25]. These theoretical and experimental works introduced the proper basis for the definition of the TG signal in water. Nevertheless they do not explore all the possible signal contributions. In particular only the thermals grating is considered neglecting the presence of other nonresonant laser excitation channels [51].

Our preliminary work [19] took into account the laser electrostrictive effect as a source forcing term in the hydrodynamic equations. This produces a pressure/density grating in the sample known as impulsive stimulated Brillouin scattering [29,34]. In that work we evaluated the complete solution of the forced hydrodynamic equations, using the lowest order wave-vector approximation. The calculated response function enables a good fit of the HD-TG signal for all the temperatures but the extraction of some hydrodynamic parameters turned out to be difficult, in particular the measurement of the ratio $\left(\frac{\partial \epsilon}{\partial T}\right)_{\rho}/\left(\frac{\partial \epsilon}{\partial \rho}\right)_{T}$.

The HD-TG data, here presented, required a more refined and extended hydrodynamic model in order to extract the water proprieties from the fit procedure. In the range of temperatures analyzed, the structural relaxation times of water (typically some picoseconds, see [5]) are always faster than the other material responses ($\approx 1/\omega_s \geqslant 1$ ns, being $\omega_s = c_s q$ the sound frequency, with c_s the adiabatic sound speed). Therefore no viscoelastic generalization of the hydrodynamic model is required. We used the standard formulation of the linearized hydrodynamic Navier-Stokes equations [40], with a Markovian approximation for the viscosity memory, measured by the longitudinal viscosity parameter $D_v=(4\eta_s/3+\eta_b)/\rho_o$ [38]. By using a Laplace transform approach, these equations can be easily solved [38], obtaining explicit expressions of $\delta\rho_q(t)$, $\delta T_q(t)$, and $\psi_q(t) = -\frac{\partial}{\partial t}[\delta\rho_q(t)/\rho_o]$ as a function of the initial values $\delta\rho_q(0)$, $\delta T_q(0)$, and $\psi_q(0)$:

$$\delta\rho_q(s) = G^{\rho\rho}\delta\rho_q(0) + G^{\rho\psi}\psi_q(0) + G^{\rho T}\delta T_q(0), \tag{6}$$

$$\delta T_q(s) = G^{T\rho}\delta\rho_q(0) + G^{T\psi}\psi_q(0) + G^{TT}\delta T_q(0), \tag{7}$$

where the fluid is assumed to be freely evolving for time $t \geqslant 0$. The same formalism can be used for the TG and LS case, remembering that, for the TG case, the results for the time evolution rigorously valid for a $\delta(t)$ excitation, should be convoluted with the actual shape of the exciting forces. The results for the Green functions are [38]

$$G^{\rho\rho} = \frac{(s+D_v q^2)(s+\gamma D_T q^2) + (\gamma-1)\omega_s^2/\gamma}{M(s)}, \tag{8}$$

$$G^{\rho T} = -\frac{\alpha\rho_o\omega_s^2}{\gamma M(s)}, \tag{9}$$

$$G^{T\rho} = -\frac{\gamma-1}{\gamma}\frac{\omega_s^2}{\alpha\rho_o}\frac{1}{M(s)}, \tag{10}$$

$$G^{TT} = \frac{s(s+D_v q^2)+\omega_s^2/\gamma}{M(s)}, \tag{11}$$

$$G^{\rho\psi} = -\rho_o\frac{s+\gamma D_T q^2}{M(s)}, \tag{12}$$

$$G^{T\psi} = -\frac{\gamma-1}{\gamma\alpha}\frac{s}{M(s)}, \tag{13}$$

where $\alpha = -(\rho_0)^{-1}\left(\frac{\partial\rho}{\partial T}\right)_P$ is the thermal expansion coefficient and the definition of the other symbols γ, D_T can be found in Table I. $M(s)=s^3+(D_v+\gamma D_T)q^2 s^2+(\omega_s^2+\gamma D_T D_v q^4)s + \omega_s^2 D_T q^2$ is the determinant of the linear system representing the hydrodynamic equations in the Laplace space.

A. Spontaneous dielectric fluctuations

In order to have a link with the early works in the literature, it is suitable to start with the case of spontaneous fluc-

TABLE I. Definition of some thermodynamic parameters with the corresponding reference, found in literature [43].

Symbol	Definition	Reference
ρ_o	mass density	[39]
γ	$=C_p/C_v$ specific heat ratio	[44,45]
C_p	specific heat	[44,45]
D_T	$=\lambda/\rho_o C_p$ thermal diffusivity, λ being the thermal conductivity	[13]
χ_T	$=\rho_0^{-1}\left(\frac{\partial\rho}{\partial P}\right)_T$ isothermal compressibility	[46]

tuation scattering. The LS signal is proportional to the Fourier transform of the dielectric correlation functions $\langle \delta\epsilon_q^*(0)\,\delta\epsilon_q(t)\rangle$, q being the wave vector fixed by experimental geometry, and $\delta\rho_q(t)$ and $\delta T_q(t)$ the spontaneous fluctuations. By using the explicit form for the Green functions, the correlator can be obtained after a proper ensemble average. This can be achieved in a simple way in the hydrodynamic limit $q\to 0$, when temperature and density fluctuations are statistically independent, $\langle \delta\rho_q(0)\,\delta T_q(0)\rangle \approx 0$. The result is

$$\begin{aligned}\langle \delta\epsilon^*(0)\,\delta\epsilon(\omega)\rangle = &\left(\frac{\partial\epsilon}{\partial\rho}\right)_T^2 \frac{1}{\pi}\langle \delta\rho^*(0)\,\delta\rho(0)\rangle \mathrm{Re}\{G^{\rho\rho}(s)\}_{s=i\omega} \\ &+ \left(\frac{\partial\epsilon}{\partial T}\right)_\rho^2 \frac{1}{\pi}\langle \delta T^*(0)\,\delta T(0)\rangle \mathrm{Re}\{G^{TT}(s)\}_{s=i\omega} \\ &+ \left(\frac{\partial\epsilon}{\partial\rho}\right)_T \left(\frac{\partial\epsilon}{\partial T}\right)_\rho \frac{1}{\pi} \\ &\times \mathrm{Re}\{\langle \delta\rho^*(0)\,\delta\rho(0)\rangle G^{T\rho}(s) \\ &+ \langle \delta T^*(0)\,\delta T(0)\rangle G^{\rho T}(s)\}_{s=i\omega},\end{aligned}$$

where we dropped the wave-vector dependence in order to simplify notations. To our knowledge, the first paper dealing with the temperature fluctuations of the dielectric constant compared with the corresponding density fluctuation was focused on the Landau-Placzek ratio of water [39]. After that, an explicit expression of the Rayleigh-Brillouin spectral density, taking into account the temperature contribution, in the limit of low damping, has been reported by Ref. [11], which was also dedicated to supercooled water. Referring now to the Green function here reported, we see that, as order of magnitude, we have from Eqs. (8)–(11) $G^{\rho\rho}\sim G^{TT}$, $G^{\rho\rho}\sim \alpha\rho_o G^{T\rho}\sim G^{\rho T}/\alpha T_o$, and thus

$$\begin{aligned}\langle \delta\epsilon^*(0)\,\delta\epsilon(\omega)\rangle = &\left(\frac{\partial\epsilon}{\partial\rho}\right)_T^2 \frac{1}{\pi}\langle \delta\rho^*(0)\,\delta\rho(0)\rangle \mathrm{Re}\{G^{\rho\rho}(s)\}_{s=i\omega} \\ &\times [1 + O(E^2/r^2) + O(E/\alpha T_o) + O(E\alpha T_o/r^2)],\end{aligned}$$

where we have introduced the dimensionless ratio between the dielectric constant derivatives [52]

$$E = \frac{T_o\left(\frac{\partial\epsilon}{\partial T}\right)_\rho}{\rho_o\left(\frac{\partial\epsilon}{\partial\rho}\right)_T} \tag{14}$$

and the ratio

$$r^2 = \frac{\langle \delta\rho^2\rangle/\rho_o^2}{\langle \delta T^2\rangle/T_o^2} = \chi_T\rho_o C_v T_o = \chi_s\rho_o C_p T_o = \frac{C_p T_o}{c_s^2}$$

between the relative mean squared fluctuation of density and temperature, given by the thermodynamic theory [41]. We thus see that in order to neglect the temperature contribution in a light-scattering experiment it is necessary to fulfill $|E| \ll r$, $|E| \ll |\alpha| T_o$, with the condition $|E\alpha| T_o/r^2 \ll 1$. In particular, the intuitive

$$\left(\frac{\partial\epsilon}{\partial T}\right)_\rho^2 \langle \delta T^2\rangle \ll \left(\frac{\partial\epsilon}{\partial\rho}\right)_T^2 \langle \delta\rho^2\rangle \tag{15}$$

(i. e., $E^2 \ll r^2$) is not sufficient, as the temperature contribution will be the dominant one when $\alpha\approx 0$ ($\gamma\approx 1$). Thus in water, around 4 °C, when the coefficient of thermal expansion is zero, the signal is dominated by the term $\left(\frac{\partial\epsilon}{\partial T}\right)_\rho \delta T$. Probably, in the case of LS the most important effect of the temperature term is a Landau-Placzek ratio $(I_c/2I_b)$ that differs from $\gamma-1$; explicit and quite involved expressions can be found in Ref. [39], but in particular, for $\alpha=0$ ($\gamma=1$) we have a particularly perspicuous expression $(I_c/2I_b)_{\alpha=0} = E^2/r^2$. A measurement of the LP ratio is hard to perform due to the spurious scattering that is inevitably present around the Rayleigh peak; nevertheless, the effect of the temperature fluctuations show clearly in the work of Ref. [39] as an excess of $(I_c/2I_b)$ over $\gamma-1$.

B. Forced dielectric modification

Let us now turn to the TG case. In a TG experiment the density and temperature changes, $\delta\rho$ and δT, are induced by the excitation laser pulses, where the relevant q wave vector is defined by the experimental geometry. In molecular liquids the variation of the dielectric constant is produced by two main channels of excitation: first, the excitation laser beams are partly absorbed generating a local heating, that in our scheme corresponds to a change $\delta T(0)$ of the local temperature; second, they create an instantaneous electrostrictive pressure, causing again a perturbation of the density derivative $\psi(0)$. Summing these terms we have

$$\begin{aligned}\delta\epsilon(t) = &\left[\left(\frac{\partial\epsilon}{\partial\rho}\right)_T G^{\rho T}(s) + \left(\frac{\partial\epsilon}{\partial T}\right)_\rho G^{TT}(s)\right]_{s\to t} \delta T(0) \\ &+ \left[\left(\frac{\partial\epsilon}{\partial\rho}\right)_T G^{\rho\psi}(s) + \left(\frac{\partial\epsilon}{\partial T}\right)_\rho G^{T\psi}(s)\right]_{s\to t} \psi(0),\end{aligned} \tag{16}$$

where the notation $s\to t$ indicates the inverse Laplace transform. Considering the orders of magnitude of the Green functions reported in Eqs. (9) and (11)–(13)), we get

$$\delta\epsilon(t) = \left[\left(\frac{\partial\epsilon}{\partial\rho}\right)_T G^{\rho T}(s)\right]_{s\to t} \{1 + O(E/\alpha T_o)\}\delta T(0) + \left[\left(\frac{\partial\epsilon}{\partial\rho}\right)_T G^{\rho\psi}(s)\right]_{s\to t} \{1 + O(E/\alpha T_o)\}\psi(0).$$

We thus see that $E \ll \alpha T_o$ is the condition for neglecting the temperature contribution. As expected, the parameter r does not enter in the δT-term visibility. $\delta T(0)$ and $\psi(0)$ are the initial conditions in the q-space determined by the absorption and the electrostrictive coefficients of the sampled matter [53].

C. TG response and signal

The dielectric modification induced by the forcing terms, Eq. (16), give us the TG signal and response function: $S^{HD} \propto R(t) \propto \delta\epsilon(t)$; here we dropped the polarization indexes since they are not relevant in the present case. Expression (16) can be cast in a more transparent format by considering the solution of the determinant $M(s)$, introduced in Eqs. (8)–(13), and performing the inverse Laplace transform of the Green functions [38]:

$$S^{HD}(t) \propto Ae^{-\Gamma t}\cos(\omega t) + Be^{-\Gamma t}\sin(\omega t) + Ce^{-\Gamma_T t}, \quad (17)$$

where A, B, C, Γ, ω, and Γ_T are functions depending on the hydrodynamic parameters appearing in Eqs. (8)–(13) and on the initial conditions forcing terms. In the approximation $q^2 D_V \ll c_s q$ and $\gamma q^2 D_T \ll c_s q$, and retaining only the lowest order in the q wave vector the A, B, and C coefficients have relative simple analytical expression [19]. Without these approximations and when all the q-orders are taken into account the analytical expressions of these coefficients are quite complicated. Furthermore, we cannot easily separate the effects of the forcing terms (electrostriction vs heating) or the presence of different dielectric modifications ($\delta\rho$-term vs δT-term). To analyze our measurements we used as a fitting function Eq. (17) with the complete definition of the coefficients, i.e., the hydrodynamics solution inclusive of all the q-vector orders. These coefficients are calculated by means of the hydrodynamic parameters following a standard numerical approach described in Ref. [42].

V. DATA ANALYSIS

To take into account the electronic fast response of the system, induced by the pump fields through a $\chi^{(3)}$-term, a $\delta(t)$ term is added to the theoretical temporal profile, Eq. (17). The resulting function is then convoluted with the experimentally determined response function of our setup, whose width $\approx$1 ns is mainly determined by the bandwidth of the detector.

The vast literature on water makes available the values of many thermodynamic parameters appearing in the hydrodynamic equations, and for almost the full temperature range analyzed. For reference, we have collected in Table I the parameters found in literature. As free parameters we adopted: (i) the adiabatic sound frequency ω_s and the viscosity parameter D_v, (ii) the initial conditions $\delta T(0)$, $\psi(0)$, (iii) the thermal diffusivity D_T, (iv) the E ratio, and (v) a further fit parameter, σ, takes into account geometrical damping of the sound, which is important when the damping rates are very small, and the acoustic oscillations die because the sound waves get out from the probing area [34]. For this reason the experimental results are fitted by using in the sound part of the Green functions an effective Gaussian envelope, i.e., by replacing the two exponential corresponding to the conjugate poles $s_\pm = \pm i\omega - \Gamma$ with $\exp(s_\pm t)\exp[-(t/\sigma)^2]$, where σ has thus the physical meaning of acoustic transit time, i. e., $c_s\sigma$ is a measure of the pump laser spot in the q-direction. As shown in Fig. 3 for two temperatures, the comparison between the data and the fit is quite good in the whole temporal range.

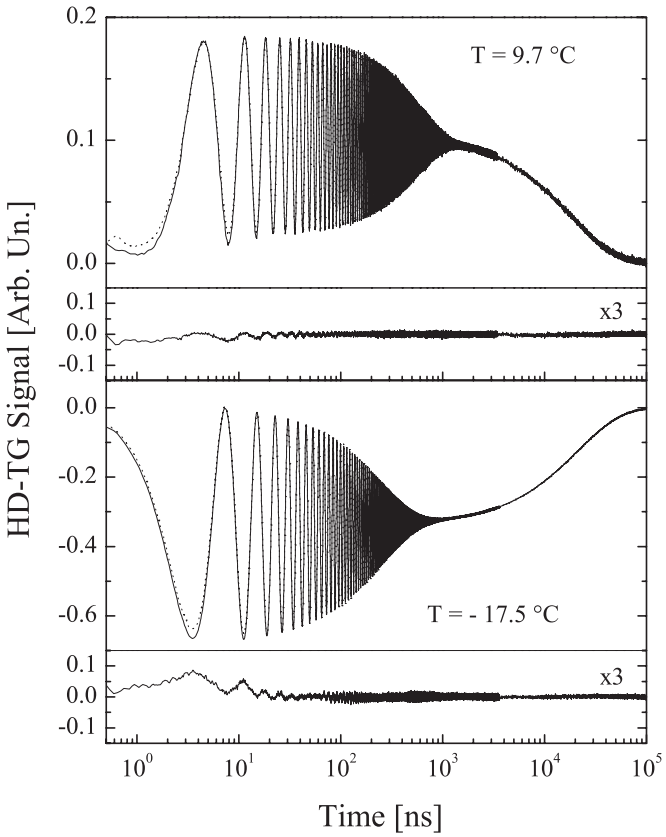

FIG. 3. Comparison between data and fit (dashed line). The fit is hardly visible, so we report also the residuals obtained by the difference between data and fit in an amplified scale.

In Fig. 4 we report the sound velocity $c_s = \omega_s/q$ obtained by our TG data vs temperature, compared to literature data [7,39,45,47,48].

In Fig. 5 we report the viscosity coefficients D_v (the corresponding acoustic damping times are simply $\tau_s \approx 1/q^2 D_v$ in the approximation $\gamma - 1 \sim 0$ [38]) vs temperature compared to literature data [7,48,49]. As shown by the scattering in the data points, the fitting procedure is able to extract a valuable damping constant as long as it reaches the acoustic transit time, defined by the interaction geometry.

Figure 6 shows the temperature behavior of the thermal diffusivity D_T (the thermal decay times are $\tau_T \approx 1/q^2 D_T$). The values corresponding to 0.8, 0.3, and −0.2 °C are not reported because the thermal decay amplitude is so weak that

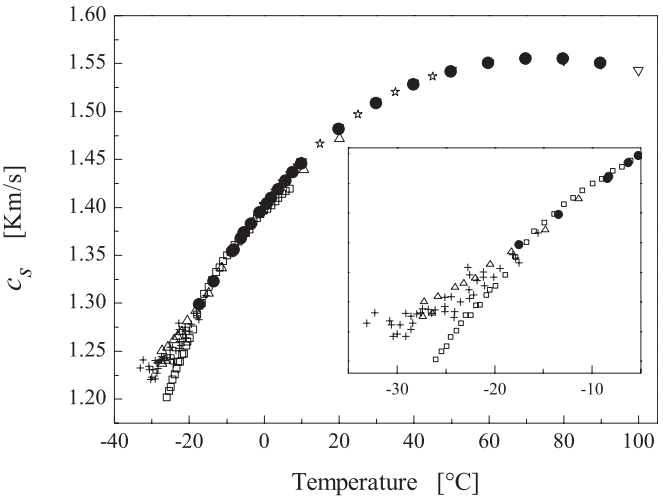

FIG. 4. Temperature dependence of the water sound velocity. Our data (●) are compared with other measurements. Ultrasonic data: at 54 KHz (+) from Ref. [47], at 925 MHz (□) from Ref. [48], and (▽) from Ref. [45]. Light scattering data: at 1.27 GHz (△) from Ref. [7] and (☆) from Ref. [39]. In the inset we report a magnification of the low temperature data, where it appears clearly the unexpected dispersion effect for ultrasonic data.

we could not extract any safe value for the parameter. The sound velocity and the thermal diffusivity, found in the present experiment, extend over a large temperature range that includes the supercooled water phase. In the overlapping temperature range a very good agreement is obtained with the literature data.

In Fig. 7 we report the fit parameter E and we compare it with its value calculated using formulas (3) and (4). The water refractive index derivatives, $\left(\frac{\partial n}{\partial T}\right)_P$ and $\left(\frac{\partial n}{\partial P}\right)_T$, have been calculated using the pressure and temperature dependence of

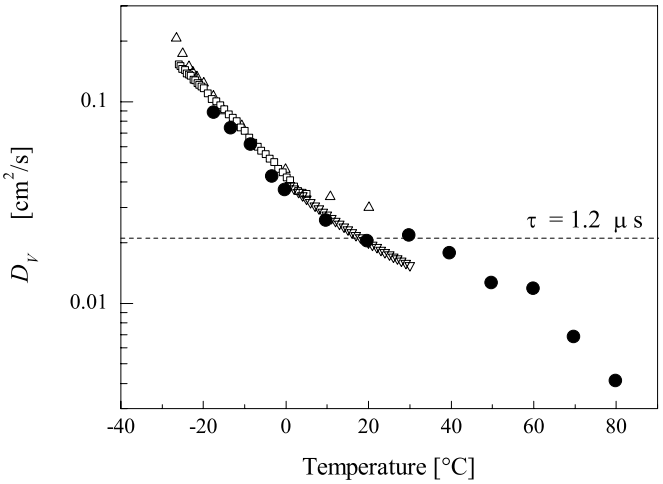

FIG. 5. Temperature dependence of the acoustic damping data. We report the viscosity coefficients D_v obtained by our fit of TG data (●), compared with the ultrasound measurements (□) from Ref. [48] and (▽) from Ref. [49]; light scattering data (△) from Ref. [7]. The dotted line represents the acoustic transit time defined by the experimental geometry, $\tau \simeq 1.2$ μs, below this limit the reported coefficients are affected by large errors.

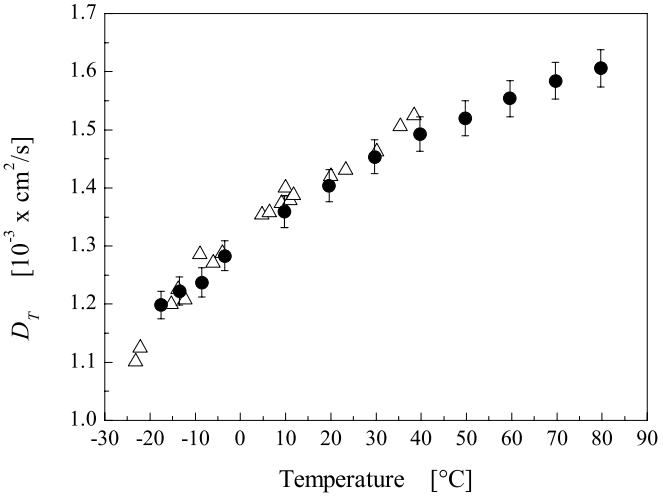

FIG. 6. Temperature dependence of the thermal diffusivity, D_T. Our data (●) are compared with data (△) from Ref. [13].

water index reported in Ref. [50]. The other thermodynamics parameters needed for this calculation have been obtained by the references quoted in Table I. The agreement is fairly good within the uncertainty estimated to be ≈20%.

VI. FINAL DISCUSSION

We performed a time-resolved HD-TG experiment in liquid and supercooled water, from −17 to 90 °C. Differently by the previous TG experiments we use pure bulk water. Indeed, the presence of solute molecules even if at low concentration level can spoil the measurement of water proprieties, in particular in the supercooled phase. The wide time window accessible enables the measurement of both the acoustic processes and the thermal diffusion dynamics, in a single experiment. The quality and extension of the measured data require an accurate hydrodynamic interpretation. So an extension of the previous hydrodynamic models has

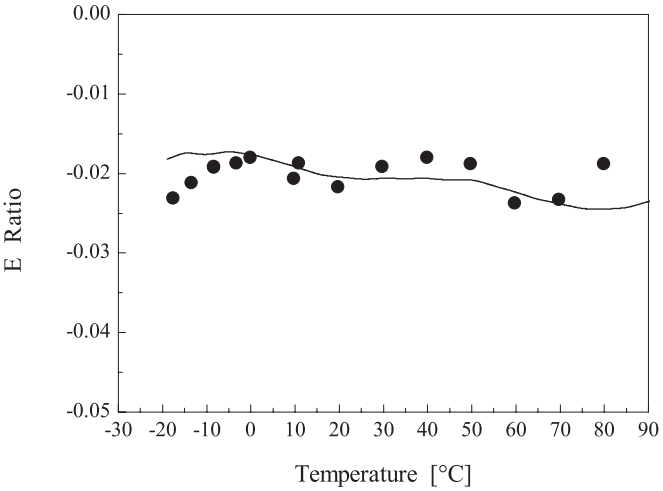

FIG. 7. Temperature dependence of the E-ratio. Our data (●) are compared with the estimate (full line) from literature data, following Eqs. (3) and (4) in the text.

been implemented and used to fit the data. This model does not use major approximations in the time/frequency or space/wave-vector scales, nor decoupling of the dynamic equations. The fitting procedure enables the measurement of many water physical parameters safely. In particular the ratio of the thermodynamic derivatives of dielectric function, E, can be directly extracted from the fit.

The water parameters measured by this single HD-TG experiment extend and confirm the previous data obtained by different experiments. The good agreement with the literature data, where existing, proves the validity of the experiment and of the model.

In particular we report the measurement of the water sound velocity for $q=0.63\ \mu\mathrm{m}^{-1}$, corresponding to a frequency of about $f=(qc_s)/2\pi\simeq 140$ MHz. Our data show a perfect agreement with data obtained from the literature, measured in a frequency range from 54 KHz to about 1 GHz. For temperatures higher than $\approx -17\ ^\circ\mathrm{C}$ the water sound velocities do not show a frequency dependence for a frequency lower than a few GHz. Conversely, the sound velocity data from literature in the deep supercooled region, below $-17\ ^\circ\mathrm{C}$, are quite misleading. In fact, the very low frequency data ($\sim$50 KHz) [47] are in very good agreement with the light scattering data [7] corresponding to a much higher frequency ($\sim$1 GHz), furthermore this data show a flattening vs the low temperature. On the other hand, other ultrasonic data [48] characterized by an intermediate frequency ($\sim$900 MHz) show a clear departure. Beside this striking discrepancy, the nature of this sound velocity flattening is not clear. Is it a dynamic or a thermodynamic phenomenon? Indeed the expected structural relaxation times τ, at that temperature, are about 10 ps corresponding to a factor $\tau\omega\sim 3\times 10^{-6}$ for a frequency of 50 KHz, making very unlikely its detection unless the strong stretching nature of the relaxation [5] plays a relevant role. The reported viscosity coefficient, D_v, does not show any dispersion effects even at the lowest temperature, proving that the damping rate scales quadratically with the q wave vector. These two results suggest a full thermodynamic nature of the peculiar temperature characteristics of the low frequency (<1 GHz) sound propagation in the supercooled water.

Our thermal diffusion data are in agreement with the previous data [13], confirming the anomalous decrease of the D_T coefficient with decreasing temperatures. Nevertheless its temperature dependence is in agreement with its classical definition, as shown in [13].

The present, low frequency, measurements of the acoustic phenomena and thermal diffusion in the supercooled phase of water confirm the anomalous temperature dependence of the characteristic properties. The sound velocity and the thermal diffusivity are in agreement with the classical thermodynamic definitions and the whole peculiar temperature dependence can be ascribed to the thermodynamic parameters (i.e., ρ, C_p, $\gamma=C_p/C_v$ and χ_T), the sound damping is also in agreement with the classical hydrodynamic definition scaling with the viscosity, as reported in [8].

Further HD-TG experiments are in progress in order to extend the water data in the lowest temperature range possible, such results could give further insights to these open problems.

ACKNOWLEDGMENTS

The research has been performed at LENS. We would like to thank R. Righini, R. M. Pick, G. Ruocco, and F. Sciortino for helpful discussion and suggestions. This work was also supported by EC Grant No. RII3-CT-2003-506350, by CRS-INFM-Soft Matter (CNR), and MIUR-COFIN-2005 Grant No. 2005023141-003. We acknowledge R. Ballerini for the accurate mechanical realizations, and M. Giuntini and M. De Pas for providing their continuous assistance in the setup of the electronics.

[1] C. A. Angell, *Water: A Comprehensive Treatise* (Plenum, New York, 1982), Vol. 7, pp. 1–814.
[2] C. A. Angell, Annu. Rev. Phys. Chem. **34**, 593 (1983).
[3] P. D. Benedetti, *Metastable Liquids* (Princeton University Press, Princeton, NJ, 1996).
[4] P. D. Benedetti, J. Phys.: Condens. Matter **15**, R1669 (2003).
[5] R. Torre, P. Bartolini, and R. Righini, Nature (London) **428**, 296 (2004).
[6] G. Ruocco and F. Sette, J. Phys.: Condens. Matter **11**, R259 (1999).
[7] S. Magazu, G. Maisano, D. Majolino, F. Mallamace, P. Migliardo, F. Aliotta, and C. Vasi, J. Phys. Chem. **93**, 942 (1989).
[8] A. Cunsolo and M. Nardone, J. Chem. Phys. **105**, 3911 (1996).
[9] C. Masciovecchio, S. C. Santucci, A. Gessini, S. D. Fonzo, G. Ruocco, and F. Sette, Phys. Rev. Lett. **92**, 255507 (2004).
[10] E. Pontecorvo, M. Krisch, A. Cunsolo, G. Monaco, A. Mermet, R. Verbeni, F. Sette, and G. Ruocco, Phys. Rev. E **71**, 011501 (2005).
[11] J. Rouch, C. C. Lai, and S. H. Chen, J. Chem. Phys. **65**, 4016 (1976).
[12] G. Maisano, P. Migliardo, F. Aliotta, C. Vasi, F. Wanderlingh, and G. D'Arrigo, Phys. Rev. Lett. **52**, 1025 (1984).
[13] O. Benchick, D. Fournier, and A. C. Boccara, J. Phys. (Paris) **46**, 727 (1985).
[14] Y. Yang and K. A. Nelson, Phys. Rev. Lett. **74**, 4883 (1995).
[15] Y. Yang and K. A. Nelson, J. Chem. Phys. **103**, 7722 (1995).
[16] Y. Yang and K. A. Nelson, J. Chem. Phys. **103**, 7732 (1995).
[17] R. Torre, A. Taschin, and M. Sampoli, Phys. Rev. E **64**, 061504 (2001).
[18] A. Taschin, R. Torre, M. Ricci, M. Sampoli, C. Dreyfus, and R. M. Pick, Europhys. Lett. **56**, 407 (2001).
[19] A. Taschin, P. Bartolini, M. Ricci, and R. Torre, Philos. Mag. **84**, 1471 (2004).
[20] A. Taschin, R. Eramo, and R. Torre, in *Time Resolved Spectroscopy in Complex Liquids*, edited by R. Torre (Springer, New York, unpublished).
[21] R. J. D. Miller, in *Time Resolved Spectroscopy*, edited by R. J. H. Clark and R. E. Hester (Wiley, New York, 1989), p. 18.

[22] M. Terazima, J. Chem. Phys. **104**, 4988 (1996).
[23] C. Glorieux, K. A. Nelson, G. Hinze, and M. D. Fayer, J. Chem. Phys. **116**, 3384 (2002).
[24] A. Taschin, P. Bartolini, M. Ricci, and R. Torre, in *Recent Advance in Ultrafast Spectroscopy, Proceedings of the XII UPS Conference*, edited by S. Califano, P. Foggi, and R. Righini, Ultrafast Processes in Spectroscopy (Leo S. Olschki, Perugia, 2003), Quaderni 21, p. 349.
[25] R. C. Desai, M. D. Levenson, and J. A. Barker, Phys. Rev. A **27**, 1968 (1983).
[26] R. M. Pick, C. Dreyfus, A. Azzimani, A. Taschin, R. Torre, M. Ricci, and T. Franosch, J. Phys.: Condens. Matter **15**, S825 (2003).
[27] R. DiLeonardo, A. Taschin, M. Sampoli, R. Torre, and G. Ruocco, Phys. Rev. E **67**, 015102(R) (2003).
[28] R. DiLeonardo, A. Taschin, M. Sampoli, R. Torre, and G. Ruocco, J. Phys.: Condens. Matter **15**, S1181 (2003).
[29] R. M. Pick, C. Dreyfus, A. Azzimani, R. Gupta, R. Torre, A. Taschin, and T. Franosch, Eur. Phys. J. B **39**, 169 (2004).
[30] T. Franosch and R. M. Pick, Eur. Phys. J. B **47**, 341 (2005).
[31] Y. R. Shen, *Principles of Non-Linear Optics* (Wiley, New York, 1984).
[32] H. J. Eichler, P. Gunter, and D. W. Pohl, *Laser-Induced Dynamic Gratings* (Spriger-Verlag, Berlin, 1986).
[33] R. W. Hellwarth, Prog. Quantum Electron. **5**, 1 (1977).
[34] Y.-X. Yan and K. A. Nelson, J. Chem. Phys. **87**, 6240 (1987).
[35] R. Torre, *Time Resolved Spectroscopy in Complex Liquids* (Springer, New York, unpublished).
[36] G. Goodno, G. Dadusc, and R. J. D. Miller, J. Opt. Soc. Am. B **15**, 1791 (1998).
[37] A. A. Maznev, K. A. Nelson, and J. A. Rogers, Opt. Lett. **23**, 1319 (1998).
[38] B. J. Berne and R. Pecora, *Dynamic Light Scattering* (Wiley, New York, 1976).
[39] C. L. O'Connor and J. P. Schlupf, J. Chem. Phys. **47**, 31 (1967).
[40] J. B. Boon and S. Yip, *Molecular Hydrodynamics* (McGraw-Hill, New York, 1980).
[41] L. D. Landau and E. M. Lifhsitz, *Statistical Physics* (Addison-Wesley, Reading, MA, 1958).
[42] M. Sampoli, A. Taschin, and R. Eramo, Philos. Mag. **84**, 1481 (2004).
[43] A useful summary of water thermodynamic data can be found at the web site: http://www.lsbu.ac.uk/water/data1.html.
[44] G. P. Johari, A. Hallbrucker, and E. Mayer, Science **273**, 90 (1996).
[45] National Institute of Standards and Technology, A gateway to the data collections. Available at http://webbook.nist.gov/chemistry (accessed December 2005).
[46] G. S. Kell, J. Chem. Eng. Data **20**, 97 (1975).
[47] E. Trinh and R. E. Apfel, J. Chem. Phys. **72**, 6731 (1980).
[48] J. C. Bacri and R. Rajaonarison, J. Phys. (Paris) **40**, L (1979).
[49] S. Hawley, J. Allegra, and G. Holton, J. Opt. Soc. Am. **47**, 137 (1970).
[50] A. H. Harvey, J. S. Gallagher, and J. M. H. Levelt-Sengers, J. Phys. Chem. Ref. Data **27**, 761 (1998).
[51] In the previous experimental works [21,22] the electrostriction phenomena is indeed introduced, but this effect is not considered in the TG signal evaluation. This is justified by the presence of solute molecules that increase substantially the laser induced heating and hence the thermal grating. In the theoretical paper by Desai *et al.* the electrostriction source is not reported at all.
[52] We would like to note that the E ratio reported in [19] was defined differently as $E=(\partial\epsilon/\partial T)_\rho/(\partial\epsilon/\partial\rho)_T$.
[53] The initial conditions, in a transient grating experiment, are created by the laser pulse interaction with matter and they define the impulsive forcing terms appearing in the hydrodynamic equations, as reported in several previous works: see, for example, page 188 of Ref [31] or page 173 of Ref. [29].